

Irrigant flow during photon-induced photoacoustic streaming (PIPS) using Particle Image Velocimetry (PIV)

Jon D. Koch¹ · David E. Jaramillo² · Enrico DiVito^{3,4} · Ove A. Peters⁵

Received: 13 March 2015 / Accepted: 4 August 2015
© Springer-Verlag Berlin Heidelberg 2015

Abstract

Objectives This study aimed to compare fluid movements generated from photon-induced photoacoustic streaming (PIPS) and passive ultrasonic irrigation (PUI).

Materials and methods Particle Image Velocimetry (PIV) was performed using 6- μm melamine spheres in water. Measurement areas were 3-mm-long sections of the canal in the coronal, midroot and apical regions for PIPS (erbium/yttrium-aluminium garnet (Er:YAG) laser set at 15 Hz with 20 mJ), or passive ultrasonic irrigation (PUI, non-cutting insert at 30 % unit power) was performed in simulated root canals prepared to an apical size #30/0.04 taper. Fluid movement was analysed directly subjacent to the apical ends of ultrasonic insert or fiber optic tips as well as at midroot and apically.

Results During PUI, measured average velocities were around 0.03 m/s in the immediate vicinity of the sides and tip of the ultrasonic file. Speeds decayed to non-measurable values at a distance of about 2 mm from the sides and tip. During PIPS, typical average speeds were about ten times higher than those

measured for PUI, and they were measured throughout the length of the canal, at distances up to 20 mm away.

Conclusions PIPS caused higher average fluid speeds when compared to PUI, both close and distant from the instrument. The findings of this study could be relevant to the debriding and disinfecting stage of endodontic therapy.

Clinical relevance Irrigation enhancement beyond needle irrigation is relevant to more effectively eradicate microorganisms from root canal systems. PIPS may be an alternative approach due to its ability to create high streaming velocities further away from the activation source compared to ultrasonic activation.

Keywords Particle image velocimetry · Photon-induced photoacoustic streaming · Ultrasonics · Endodontics · Irrigation

✉ Ove A. Peters
opeters@pacific.edu

¹ Department of Mechanical and Aerospace Engineering, Allen School of Engineering, Trine University, Angola, IN, USA

² Department of Endodontics, University of Texas Health Science Center at Houston, School of Dentistry, Houston, TX, USA

³ Private Practice, Arizona Center for Laser Dentistry, Scottsdale, AZ, USA

⁴ Arizona School of Dentistry and Oral Health, Mesa, AZ, USA

⁵ Department of Endodontics, University of the Pacific Arthur A. Dugoni School of Dentistry, 155 5th St, San Francisco, CA 94103, USA

Introduction

An important aim of root canal treatment is the elimination or prevention of periradicular periodontitis; it is well established that bacteria and their toxins are the cause of this disease [13] and therefore eradication, or at least reduction to a biologically acceptable number, of intracanal microorganisms is required [23]. Enlargement of root canals with current root canal instruments reduces bacterial counts even in the case of buccolingually wide root canals [24]. However, preparation does not eliminate all microorganisms from the root canal system. Therefore, antimicrobial irrigants are commonly used and it is believed that enhancement of the flushing action is effective in improving root canal cleanliness [2, 11]. Different agitation techniques have been proposed to improve the efficacy of irrigation solutions, including agitation with hand

files, gutta-percha cones, plastic instruments and sonic and ultrasonic devices [9].

Lasers have been explored as a means to enhance endodontic treatment procedures in a variety of ways in addition to enhance irrigation efficacy. One of the more recent suggestions is the use of laser energy to enhance irrigation. Lasers may be used directly to irradiate radicular walls [28] or to activate photosensitizers that associate with bacteria [8]. Both of these approaches have failed to consistently promote bacteria-free root canal systems in vitro [19, 28].

More recent work proposed to activate irrigation solutions by the transfer of pulsed laser energy [3, 7]. Irrigation enhanced by erbium/yttrium-aluminium garnet (Er:YAG) laser light appears to be effective in removing dentin debris [3] and smear layer [5]. Specifically, the action of a pulsed Er:YAG laser via photon-induced photoacoustic streaming (PIPS) has been shown to be effective in root canal debridement [5, 10, 21].

However, to the best of our knowledge, the detailed nature of the streaming patterns that permit PIPS to disinfect root canals has not been established.

Particle Image Velocimetry (PIV) is a non-intrusive technique for the measurement of a velocity field [22]. The displacement of small tracer particles added to a fluid is recorded by high-speed imaging and analysed using statistical correlation methods to extract the velocity distribution in the examined plane [22].

The aim of the present study was to compare differences in fluid movement generated from PIPS and passive ultrasonic irrigation (PUI) in a curved simulated root canal. Particle Image Velocimetry measurements were performed to assess the magnitude and distribution of the irrigant flow velocity stimulated by PIPS device inside a simple specimen and to compare flow created with an ultrasonic device under experimental conditions that simulated clinical use.

Materials and methods

An acrylic endodontic training block (Viade Products, Camarillo, CA, USA) with a simulated root canal was instrumented to a size #30/0.04 by using Vortex rotary files (Dentsply Tulsa Dental, Tulsa, OK, USA) in a crown-down technique. The canal was irrigated with distilled water by using a syringe and a 30-g irrigation needle and then dried with paper points. The prepared block was clamped to a translation stage to control its location. After needle injection of the water/particle mixture as described below, one of the two tested irrigation devices was placed into the canal (PIPS laser fibre or passive ultrasonic irrigation tip as described below). The respective tip was secured in position using a clamping device; the tip of the PIPS fibre was inserted to a depth of about 3 mm below the top of the plastic block while the ultrasonic instrument (K file

size #15, Satelec-Acteon, Merignac, France) was inserted 3 mm below the top of the orifice of the canal with the tip being visible (section a, Fig. 1). This depth was sufficient to ensure the activation of the fluid within the canal but not so deep as to allow the instrument to bind against the canal wall. The location of each instrument is indicated by the outlines in Figs. 1 and 2. The ultrasonic instrument was connected to a Spartan USA Endo-1 unit (Obtura Spartan, Algonquin, Chicago, IL, USA) at an intensity setting of 3 (on a scale of 0 to 10). The light source for the PIPS tip was an Er:YAG laser (2940 nm) set to 20 mJ, 15 Hz and a 50- μ s pulse duration. The fibre tip was tapered and stripped; it had a diameter of 600 μ m (LightWalker AT, Fotona, Ljubljana, Slovenia).

The PIV configuration is described in detail elsewhere [15]; in brief, a double-pulsed, frequency-doubled YAG laser (Solo PIV; New Wave Research, Sunnyvale, CA, USA) was used as the excitation source. The beam was expanded, steered and focused through a $\times 5$ microscope objective onto the root canal model that was filled with a mixture of dye-coated microparticles (6-mm melamine resin particles coated with rhodamine B, Fluka, #74,097, Buchs, Switzerland) and distilled water. Fluorescence was captured through the objective lens and focused onto a CCD camera (LaVision Imager

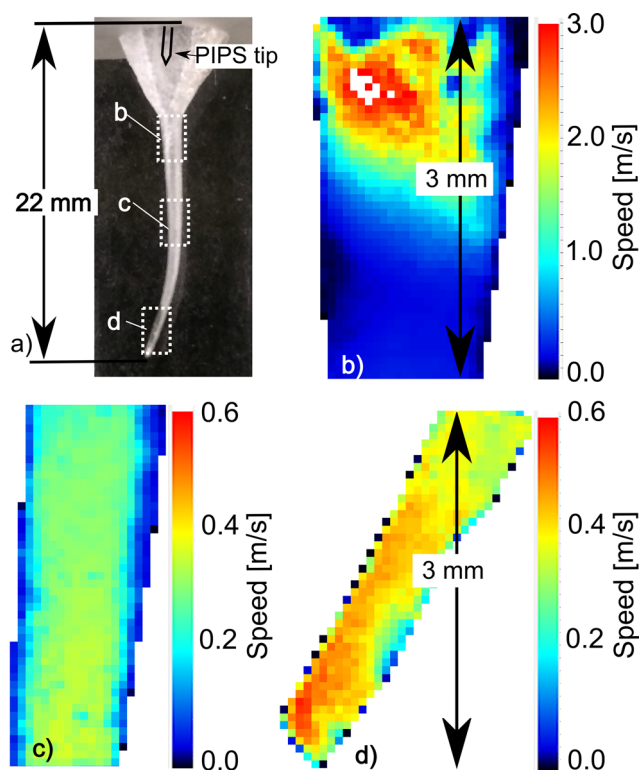


Fig. 1 Image (a) at top left shows entire canal model and locations where PIV measurements were made with methods detailed in an earlier publication [24]. Images (b), (c), (d) show average speeds from at least 100 PIV measurements taken 0.8 ms after a 15 mJ PIPS laser pulse in the locations indicated by boxes in (a). The velocity scale for each image is indicated by the colour bar on the right. The PIPS tip was located at the top of the coronal third for each measurement as outlined in the left hand image

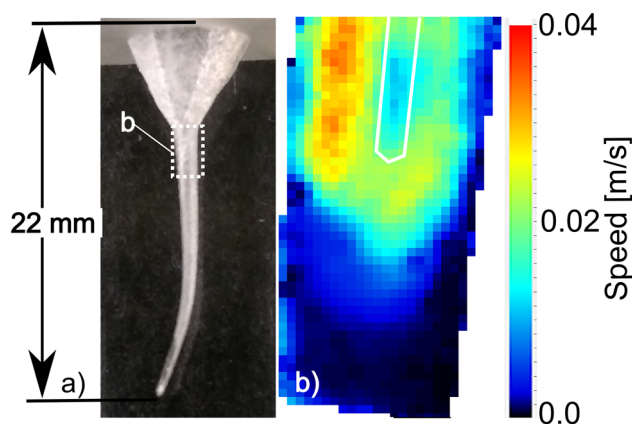


Fig. 2 Image at left (a) shows the canal model and in box (b) the location where velocity measurements were made with the ultrasonic file inserted into the top of the canal. The position of the end of the non-activated file (behind the PIV image plane) is shown as a *white outline* in the image on the right. Image on the right (b) shows the average speed around the file from 200 PIV measurements taken during activation of the file in a static position. Average speeds immediately around the file are approximately 0.03 m/s. The average speed decays to less than 0.01 m/s within a distance of 2 mm below the file (the *bottom* of the image on the right). There was no observable fluid movement in lower sections of the canal model

Pro X 2 M; LaVision, Göttingen, Germany). Non-fluorescent light was rejected using a dichroic reflector and band-pass filter.

When the ultrasonic file was studied, images were separated in time by 150 μ s. This time corresponds to slightly more than four periods of ultrasonic oscillation; the measurements are thus suitable for capturing the average velocities around the file but not the velocity of the file itself or of the oscillatory components that have been noted in the area immediately adjacent to the file [27]. The ultrasonic file was turned on approximately 1 s before images were acquired in a free-running mode without regard to synchronization. When the PIPS tip was studied, images were separated by 75 μ s in the lower section of the canal (Fig. 1, sections c and d) but separated by 15 μ s in the upper section of the canal because the velocities in the upper section were found to be much faster than other locations. All PIPS images were synced to a time that was 0.8 ms after the firing of the laser. Synchronization between the image acquisition and the PIPS laser was accomplished by detecting a signal from the PIPS laser flashlamp using a fast photodiode (Thorlabs, DET10A, 2 ns response time, Newton, NJ, USA) and monitoring on an oscilloscope. The period and delay of the PIV system, which was also monitored on the oscilloscope, was then adjusted to match the free-running PIPS laser.

Sets of image pairs were cross-correlated using DaVis 7.1 (LaVision). Initial interrogation windows were 128 pixels on a side. Based on 1/4 of this window size, the maximum measurable velocity component was approximately 0.4 m/s for PUI and 0.8 m/s for PIPS (4 m/s in the upper region of Fig. 1a). The minimum measurable velocity component based

on a conservative 0.5 pixel detectable displacement was about 0.005 m/s for PUI and 0.01 m/s for PIPS (0.05 m/s in the upper region). These minimum measurable velocities serve as estimates of the measurement uncertainty. Multipass processing was used, ultimately resulting in vectors corresponding to 64-pixel windows with 50 % overlap, or 1 vector every 0.06 mm. The results of 200 vector images were averaged for PUI irrigation (Fig. 2, discussed below), while the PIPS measurements were averaged over at least 100 vector images (Fig. 1, discussed below). Syncing the PIV measurement with the PIPS laser required to start recording images in a non-synced mode while adjusting the PIV-PIPS timing; these non-used images consumed some of the available RAM in the computer memory, resulting in fewer images available for PIPS measurements.

Reynolds number

The measured speeds in each region were averaged over space and time to obtain a single ensemble-averaged velocity. A Reynolds number, Re , was then calculated based on the density ($\rho = 998 \text{ kg/m}^3$) and viscosity ($\mu = 0.955 \text{ g/m s}$) of water at 22 °C and the ensemble-average speeds (v) in each PIPS region as follows:

$$Re = \frac{\rho v D}{\mu}$$

The characteristic dimension, D , was the average canal diameter in each imaged region.

Results

Photon-induced photoacoustic streaming

Figure 1 shows that large average fluid speeds ($> 3 \text{ m/s}$) are present in the coronal portion of the canal (Fig. 1b). Average fluid speeds are somewhat slower in the middle of the canal (Fig. 1c) but still significant (approx. 0.3 m/s) and fairly uniform over the imaged region. Average speeds in the apical region (Fig. 1d) are nearly the same as in the middle of the canal (0.3–0.5 m/s). Ensemble (spatial and temporal) averaging was performed to obtain characteristic speeds at each measured location as shown in Fig. 1. From top to bottom, the spatially and temporally averaged speeds were 1.02, 0.25, and 0.43 m/s, respectively. These correspond to Reynolds numbers of approximately 1670 (coronal third), 290 (midroot) and 280 (apical), respectively. As a means of describing the width of the speed distribution, the standard deviations of the measured speeds in each region were 1.25 m/s in the coronal region, 0.19 m/s in the midroot and 0.28 m/s in the apical region.

Individual images indicate the presence of large-scale vertical motions in the mid and lower portions of the canal. Example instantaneous images of the PIPS flow in the apical region are shown in Fig. 3. At the moment of measurement, these flow fields could be dominated by flow in either the upward (Fig. 3a, c) or the downward (Fig. 3b, d) direction, likely a result of the highly unsteady nature of the flow and the variability in the timing between the fluid motion and the flashlamp output. Occasional vortical structures (top of Fig. 3a) and regions of apparent low velocities were also noted; areas of large changes in velocity over a short distance indicate the presence of shear stresses.

Passive ultrasonic irrigation

For PUI, Fig. 2 shows the average speed around the file from 200 PIV measurements taken during activation of the file in a static position (Fig. 2a). Average speeds around the file are approximately 0.03 m/s, only about one tenth the value of those observed throughout the canal during the PIPS experiments. Furthermore, the average speed decays to less than 0.01 m/s within a distance of 2 mm below the file (the bottom of the image on the right). There was no observable fluid movement in lower sections of the canal model.

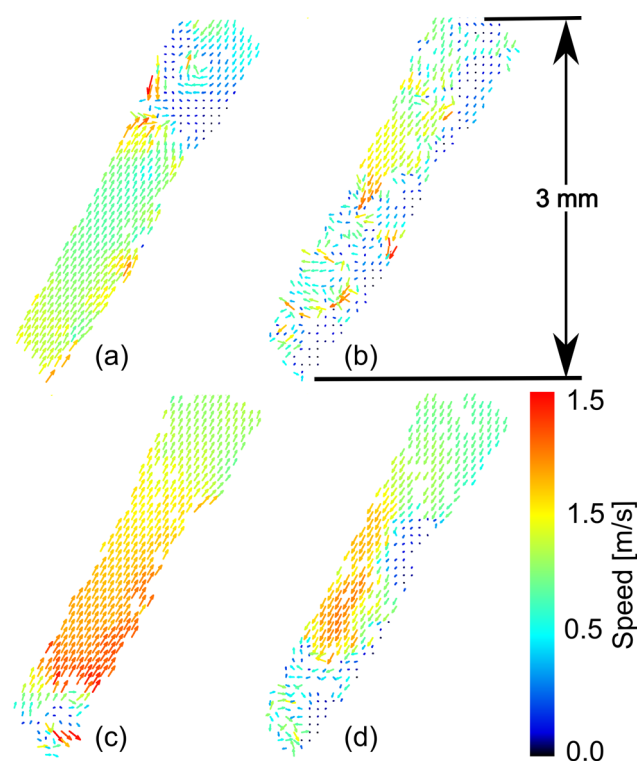


Fig. 3 Single-measurement images of PIPS velocity fields in the apical region. Large-scale axial flows are occasionally present and are noted to be travelling in each direction (a, c). Some vortical motions are noticeable (top of a). Jet-like structures are also found (b, d)

Discussion

In this study, irrigant fluid speeds were assessed by PIV, comparing laser-activated irrigation (PIPS) and passive ultrasonic irrigation (PUI). Fluid movement measured distant from the PIPS tip was evident, compared to the lack of obvious movement much past 1 mm below an ultrasonic tip. Since the estimated measurement uncertainty of a PIPS PIV data point was ± 0.05 m/s while that of the PUI experiment was ± 0.005 m/s, the differences between the ensemble-averaged velocity in the midroot region (0.25 m/s) and the speed near the PUI instrument (0.03 m/s) are significantly outside the measurement uncertainty. Hence, PIPS was associated with a significantly greater average speed than PUI by at least a factor of 10.

Notably, at small distances below the tip the overall fluid velocities with PIPS were about ten times higher than those predicted from numerical simulation [1, 25] for side-vented needles, at similar distances from the needle tip. These velocities relate to the experimental conditions, with plastic rather than dentin as surface and absolute numbers in actual root canal systems will likely vary.

The Reynolds numbers, if compared to transitional regimes in pipe flow, would tend to indicate laminar flow; however, given the unsteady nature of this flow and the oscillations noted in single images, we would suggest a classification of a transitional flow for at least a portion of the time after the PIPS laser pulse.

It is interesting to note that the ensemble-averaged speed appears to increase in the apical region relative to the midroot section (0.43 m/s in the apical compared to 0.25 m/s in the midroot). Passive ultrasonic irrigation typically results in a decay in the velocity field as one moves away from the excitation source [26]. Possible reasons for this observation include the existence of localized resonance between the excitation field and the flow field inside the cavity as well as statistical uncertainty in the samples collected. Resonance may exist in some areas inside the canal due to the superposition of pressure waves and their impact on the velocity field.

It is also possible that the samples, obtained via the two-dimensional interrogation of a three-dimensional flow field that oscillates rapidly in time, are not sufficiently representative of the averaged ensemble speed. As indicated by the substantial standard deviations of 0.19 m/s in the midroot and 0.28 m/s in the apical region, however, there is significant overlap between the distributions. Further studies on how the flow field evolves after a single PIPS laser pulse are needed to address this question.

Ultrasonic irrigation is thought to act via a process commonly referred to as acoustic streaming; recently, it was suggested that some cavitation may also occur [18]. Regardless, its efficacy depends on the ability of the activated instrument to oscillate [26] freely within the canal, and its action may thus be restricted or reduced in curved or small canals. The

inability to freely oscillate may be a reason that PUI had only limited effect in removing bacterial burden from bacterially contaminated small canals in vitro [21]. In the present experimental configuration, the PUI file was inserted only to a distance of 3 mm into the curved root canal in order to ensure there would be no binding of the file against the side. The induced flow field around the tip of the file is thus thought to be uninhibited by binding effects and is qualitatively similar to studies where the file has been fully inserted into a model canal in a non-binding configuration.

PIPS is believed to cause fluid motion via pressure waves that propagate outward from expanding and collapsing cavitation bubbles at the PIPS tip [6]. The size, shape and dynamic behaviour of the bubble are controlled by the shape of the tip and settings of the Er:YAG laser [5]. In this study, sub-ablative parameters were used to produce the cavitation bubble [3–5]. That is to say, the high absorption of the Er:YAG wavelength by water combined with the high peak power derived from the short pulse (50 μ s) resulted in the rapid formation, expansion and subsequent collapse of a vapour bubble at the tip rather than any direct material removal at the edge of the canal. The rapid movement of the fluid around the tip propagates to the surrounding fluid, thus causing the PIPS effect.

The data in this study indicate that PIPS induces larger average speeds in the fluid within a model canal, compared to ultrasonic activation [16] and it does so at a significant distance from the instrument. Effective clinical irrigation is thought to originate from a combination of fluid dynamic or mechanical forces and chemistry. The velocity field is arguably the most important variable needed to characterize the shear stresses and bulk transport within the canal from a fluids perspective. Hence, the large difference in speeds between the two instruments is suggestive of a clinical advantage for the disinfection and possible biofilm detachment in the main root canal. However, this does not address dentinal tubule contamination and different experiments will be necessary to test the effect of irrigation activation in this condition.

To the best of our knowledge, direct clinical comparisons between the two irrigation techniques tested here in vitro are not yet available. However, other studies can lend some insight; it has been reported that shear forces of up to 2.8 N/m² were generated with plastic finishing files designed for irrigation enhancement [14]. This is comparable to findings on continuous application of ultrasonic activation [16]. Of note, these values would appear to be too low to completely detach biofilm from substrate; for example, Huang et al. [12] indicated that up to 46 N/m² is needed to detach *Pseudomonas aeruginosa* from silicone material. Layton et al. found that *Enterococcus faecalis* biofilm in plastic models was reduced but not eliminated after continuous ultrasonic activation [16].

Shear-stress measurements are not available for PIPS, but Ordinola-Zapata et al. demonstrated the superior ability of

PIPS-supported irrigation to disrupt biofilm on dentin substrate [20]. Likewise, debris was more effectively removed from root canal systems in vitro with laser-activated PIPS irrigation, compared to needle irrigation [17]. Further experiments could be designed to test different canal shapes that, within the limits of canal anatomy and available preparation techniques, could promote optimized fluid movement.

In conclusion, our findings suggest that PIPS-induced fluid movement is more prominent at a distance compared to ultrasonic irrigation. To extend the findings of this using PIV, more experiments under varied conditions should be performed to better understand streaming patterns of current irrigation modalities under clinical conditions.

Conflict of interest This project was financially supported by Medical Dental Advance Technologies Group, of which Dr. DiVito is a partner.

References

1. Boutsoukias C, Verhaagen B, Versluis M, Kastrinakis E, v.d. Sluis L (2010) Irrigant flow in the root canal: experimental validation of an unsteady computational fluid dynamics model using high-speed imaging. *Int Endod J* 43:393–403
2. Burleson A, Nusstein J, Reader A, Beck M (2007) The in vivo evaluation of hand/rotary/ultrasound instrumentation in necrotic, human mandibular molars. *J Endod* 33:782–787
3. de Groot SD, Verhaagen B, Versluis M, Wu MK, Wesselink PR, van der Sluis LW (2009) Laser-activated irrigation within root canals: cleaning efficacy and flow visualization. *Int Endod J* 42:1077–1083
4. de Moor RJG, Meire M, Gokharkey K, Moritz A, Vannobbergen J (2010) Efficacy of ultrasonic versus laser-activated irrigation to remove artificially placed dentin debris plugs. *J Endod* 36:1580–1583
5. DiVito E, Peters OA, Olivi G (2012) Effectiveness of the erbium: YAG laser and new design radial and stripped tips in removing the smear layer after root canal instrumentation. *Lasers Med Sci* 27: 273–280
6. Doukas AG, Flotte TJ (1996) Physical characteristics and biological effects of laser-induced stress waves. *Ultrasound Med Biol* 22: 151–164
7. George R, Meyers IW, Walsh LJ (2008) Laser activation of endodontic irrigants with improved conical laser fiber tips for removing smear layer in the apical third of the root canal. *J Endod* 34:1524–1527
8. George S, Kishen A (2007) Advanced noninvasive light-activated disinfection: assessment of cytotoxicity on fibroblast versus antimicrobial activity against *Enterococcus faecalis*. *J Endod* 33:599–602
9. Gu LS, Kim JR, Ling J, Choi KK, Pashley DH, Tay FR (2009) Review of contemporary irrigant agitation techniques and devices. *J Endod* 35:791–804
10. Gunesser MB, Arslan D, Usumez A (2015) Tissue dissolution ability of sodium hypochlorite activated by photon-initiated photoacoustic streaming technique. *J Endod* 41:729–732
11. Gutarts R, Nusstein J, Reader A, Beck M (2005) In vivo debridement efficacy of ultrasonic irrigation following hand-rotary instrumentation in human mandibular molars. *J Endod* 31:166–170

12. Huang Z, McLamore E, Chuang H, Zhang W, Wereley S, Leon J, Banks M (2013) Shear-induced detachment of biofilms from hollow fiber silicone membranes. *Biotechnol Bioeng* 110:525–534
13. Kakehashi S, Stanley HR, Fitzgerald RJ (1965) The effects of surgical exposures of dental pulps in germ-free and conventional laboratory rats. *Oral Surg Oral Med Oral Path* 20:340–349
14. Koch J, Borg J, Matteson A, Olsen F, Bahcall J (2012) An in vitro comparative study of intracanal fluid motion and wall shear stress induced by ultrasonic and polymer rotary finishing files in a simulated root canal model. *ISRN Dent* 2012:764041
15. Koch J, Smith N, Garces D, Gao L, Olsen F (2014) In vitro particle image velocity measurements in a model root canal: flow around a polymer rotary finishing file. *J Endod* 40:412–416
16. Layton G, Wu W-I, Selvaganapthy RR, Friedman S, Kishen A (2015) Fluid dynamics and biofilm removal generated by syringe-delivered and two ultrasonic-assisted irrigation methods: a novel experimental approach. *J Endod* 41:884–889
17. Lloyd A, Uhles JP, Clement DJ, Garcia-Godoy F (2014) Elimination of intracanal tissue and debris through a novel laser-activated system assessed using high-resolution micro-computed tomography: a pilot study. *J Endod* 40:584–587
18. Macedo R, Verhaagen B, Rivas DF, Versluis M, Wesselink P, v. d. Sluis LW (2013) Cavitation measurement during sonic and ultrasonic activated irrigation. *J Endod* 40:580–583
19. Meire MA, De Prijk K, Coenye T, Nelis HJ, De Moor RJG (2009) Effectiveness of different laser systems to kill *Enterococcus faecalis* in aqueous suspension and in an infected tooth model. *Int Endod J* 42:351–359
20. Ordinola-Zapata R, Bramante CM, Aprecio RM, Handysides R, Jaramillo DE (2014) Biofilm removal by 6 % sodium hypochlorite activated by different irrigation techniques. *Int Endod J* 47:659–666
21. Peters OA, Bardsley S, Fong J, Pandher G, Divito E (2011) Disinfection of root canals with photon-initiated photoacoustic streaming. *J Endod* 37:1008–1012
22. Raffel M, Willert CE, Kompenhans J (1998) Particle image velocimetry: a practical guide. Springer, Berlin, Heidelberg
23. Ricucci D, Siqueira JF (2010) Fate of the tissue in lateral canals and apical ramifications in response to pathologic conditions and treatment procedures. *J Endod* 36:1–15
24. Siqueira JF, Alves FRF, Almeida BM, de Oliveira JCM, Rocas IN (2010) Ability of chemomechanical preparation with either rotary instruments or self-adjusting file to disinfect oval-shaped root canals. *J Endod* 36:1860–1865
25. Snjaric D, Carija Z, Braut A, Halaji A, Kovacevic M, Kuis D (2012) Irrigation of human prepared root canal—ex vivo based computational fluid dynamics analysis. *Croat Med J* 53:470–479
26. v. d. Sluis LW, Versluis M, Wu MK, Wesselink PR (2007) Passive ultrasonic irrigation of the root canal: a review of the literature. *Int Endod J* 40:415–426
27. Verhaagen B, Boutsoukis C, van der Sluis LW, Versluis M (2014) Acoustic streaming induced by an ultrasonically oscillating endodontic file. *J Acoust Soc Am* 135:1717–1730
28. Yasuda Y, Kawamorita T, Yamaguchi H, Saito T (2010) Bactericidal effect of Nd:YAG and Er:YAG lasers in experimentally infected curved root canals. *Photomed Laser Surg* 28:S75–S78